

## Euler force actuation mechanism for siphon valving in compact disk-like microfluidic chips

Yongbo Deng, Jianhua Fan, Song Zhou, Teng Zhou, Junfeng Wu, Yin Li, Zhenyu Liu, Ming Xuan, and Yihui Wu

Citation: *Biomicrofluidics* **8**, 024101 (2014); doi: 10.1063/1.4867241

View online: <http://dx.doi.org/10.1063/1.4867241>

View Table of Contents: <http://scitation.aip.org/content/aip/journal/bmf/8/2?ver=pdfcov>

Published by the [AIP Publishing](#)

---

### Articles you may be interested in

[Direct measurement of the dielectrophoresis forces acting on micro-objects using optical tweezers and a simple microfluidic chip](#)

*Appl. Phys. Lett.* **105**, 103701 (2014); 10.1063/1.4895115

[A pneumatic valve controlled microdevice for bioanalysis](#)

*Biomicrofluidics* **7**, 054116 (2013); 10.1063/1.4826158

[Hand-powered microfluidics: A membrane pump with a patient-to-chip syringe interface](#)

*Biomicrofluidics* **6**, 044102 (2012); 10.1063/1.4762851

[Excimer laser fabrication of polymer microfluidic devices](#)

*J. Laser Appl.* **15**, 255 (2003); 10.2351/1.1585085

[Responsive biomimetic hydrogel valve for microfluidics](#)

*Appl. Phys. Lett.* **78**, 2589 (2001); 10.1063/1.1367010

---



## Euler force actuation mechanism for siphon valving in compact disk-like microfluidic chips

Yongbo Deng, Jianhua Fan, Song Zhou, Teng Zhou, Junfeng Wu, Yin Li, Zhenyu Liu, Ming Xuan, and Yihui Wu<sup>a)</sup>

*State Key Laboratory of Applied Optics, Changchun Institute of Optics, Fine Mechanics and Physics (CIOMP), Chinese Academy of Sciences, Changchun China, 130033*

(Received 17 January 2014; accepted 19 February 2014; published online 5 March 2014)

Based on the Euler force induced by the acceleration of compact disk (CD)-like microfluidic chip, this paper presents a novel actuation mechanism for siphon valving. At the preliminary stage of acceleration, the Euler force in the tangential direction of CD-like chip takes the primary place compared with the centrifugal force to function as the actuation of the flow, which fills the siphon and actuates the siphon valving. The Euler force actuation mechanism is demonstrated by the numerical solution of the phase-field based mathematical model for the flow in siphon valve. In addition, experimental validation is implemented in the polymethylmethacrylate-based CD-like microfluidic chip manufactured using CO<sub>2</sub> laser engraving technique. To prove the application of the proposed Euler force actuation mechanism, whole blood separation and plasma extraction has been conducted using the Euler force actuated siphon valving. The newly introduced actuation mechanism overcomes the dependence on hydrophilic capillary filling of siphon by avoiding external manipulation or surface treatments of polymeric material. The sacrifice for highly integrated processing in pneumatic pumping technique is also prevented by excluding the volume-occupied compressed air chamber. © 2014 AIP Publishing LLC. [<http://dx.doi.org/10.1063/1.4867241>]

### I. INTRODUCTION

Compact disk (CD)-like microfluidic chips, using forces produced by rotating platforms to drive microfluidic flows, integrate a comprehensive set of laboratory unit operations including metering, mixing, diluting, reagent storage, and cell lysis. The problem is on the integration of micropump in microfluidic chips. However, this problem was avoided effectively by the centrifugal force in CD-like microfluidic chips. Thus, the CD-like microfluidic chip has been studied thoroughly and emerged as a unique approach to the development of integrated total analysis systems for medical diagnostics.<sup>1-4</sup>

In CD-like microfluidic chips, siphon valve is one key component used for extraction and metering operation of the liquid phase.<sup>2,5</sup> As presented in Refs. 2 and 5, spontaneous capillary flow is required before rotation of the centrifugal platform and induction of the siphonal flow in siphon valve. Spontaneous capillary flow allows the manipulation of fluids back to the center of the CD-like chip to fill the siphon and actuate the siphon valving. In polymeric microfluidic chips, spontaneous capillary flow requires the hydrophilicity of the material. However, as common polymers are innately hydrophobic, capillary flow is induced (transiently) either by plasma treatment or, more stably, by depositing coatings. Hydrophilization induced by plasma treatment fades eventually, thereby causing reduced and irreproducible wicking behaviour. Thus, the long-term stability of the CD-like chip cannot be ensured. Meanwhile, hydrophilic coating steps have the problem with regard to increasing the cost and complexity of device manufacture and assembly.<sup>4</sup>

---

<sup>a)</sup>Electronic mail: yihuiwu@ciomp.ac.cn

To avoid the surface treatment and external manipulation of plastics, several new actuation mechanisms have been proposed to optimize the use of real estate on a CD-like chip. These new mechanisms include pneumatic pumping,<sup>6,7</sup> suction-enhanced,<sup>8</sup> and supernatant decanting methods.<sup>9</sup> As pointed out in Ref. 3, pneumatic pumping is typically not practical for highly integrated processing because of the extra compressed air chamber. The suction-enhanced mechanism has strict requirement on the size and shape of the microchannels. In the novel supernatant decanting method, the siphon valve is avoided and the decanting is performed based on the deformation of plastic lids and reasonable choice of the rotational direction and deceleration.<sup>9</sup> However, the siphon valve is prone to be unavoidable for the extraction of liquid after some operation, e.g., the shake mode mixing.<sup>10</sup> Other available active-pumping<sup>11–14</sup> and ic-valving<sup>15</sup> methods have the drawbacks on raising the complexity of systems.

Using the Euler force produced in the acceleration of rotating platform, this paper proposes an actuation method for the siphon valving, to avoid the unstable surface treatment and complicated external manipulation of plastics and optimize the use of real estate on a CD-like chip as well as allow for large-scale system integration which was not practical for pneumatic pumping. The paper is organized as follows: the methodology of the Euler force actuation mechanism is introduced for the siphon valving in Sec. II; the Euler force actuated siphon valving is modeled mathematically based on the phase-field method in Sec. III; the numerical analysis is performed in Sec. IV using the finite element method; the experimental method is presented in Sec. V; numerical and experimental results and the corresponding discussion are provided in Sec. VI; the application of the proposed Euler force actuated siphon valving is conducted for whole blood separation and plasma extraction in Sec. VII; and the paper is concluded in Sec. VIII.

## II. METHODOLOGY

The siphon valve, used for separating, extracting, metering, etc., is formed by a siphon with two chambers, respectively, connected to the inlet and outlet of the siphon, as shown in Fig. 1. Conventionally, siphon valving of liquid requires two separate rotations of the CD-like chip and one long-enough stop between these two separate rotations (Fig. 2). In the first rotation, the liquid in the sample chamber is driven into the metering chamber by the centrifugal force and the excessive liquid overflows into the waste chamber as shown in Fig. 2(b); during the rotation stop, capillary fills the siphon with the operated liquid (Fig. 2(c)); in the second rotation, siphonal flow is produced by the centrifugal force and the liquid in the metering chamber with rotating radius shorter than that of the siphon inlet is extracted into the extracting chamber (Fig. 2(d)). Designing the siphon valve requires that rotating radius of the siphon

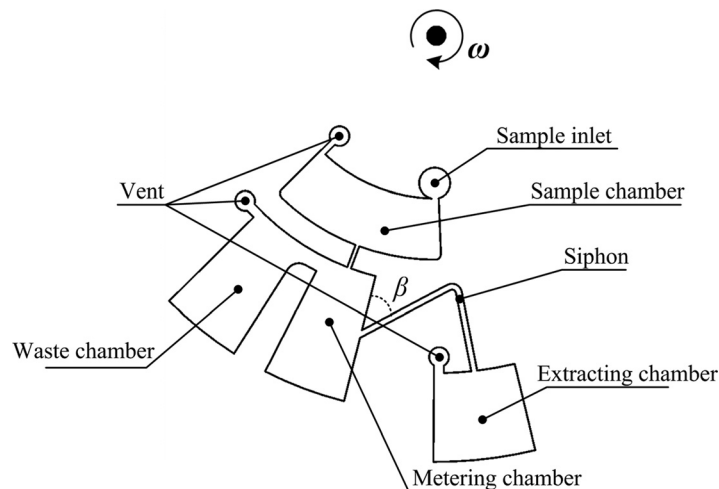


FIG. 1. Schematic for the siphon valve in a CD-like microfluidic chip, where  $\beta$  is the inclination angle of the siphon channel.

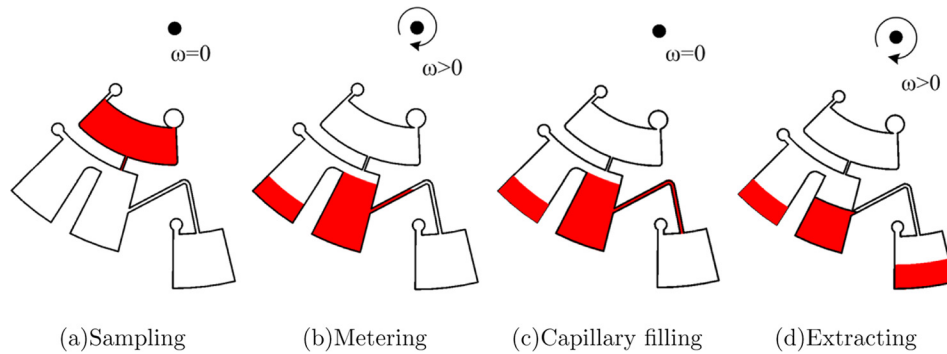


FIG. 2. Conventional operation of liquid in the siphon valve based on capillary filling of the siphon.

outlet is longer than that of the inlet, and rotating radius of the siphon crest point is shorter than that of the liquid surface formed by the first rotation in the metering chamber. Capillary filling is key for the liquid operation in a siphon valve and the long-term stability of the CD-like microfluidic chip. However, the instability of spontaneous capillary flow is typically an obstacle, particularly for the microfluidic chip fabricated using polymers with inherent hydrophobicity.

To overcome the dependence on capillary filling, this paper introduces a new actuation mechanism for the siphon valve based on the Euler force loaded on the fluid during the acceleration of a CD-like microfluidic chip. Euler force, corresponding to the Euler acceleration, is a fictitious force produced during the acceleration of the rotating system.<sup>16</sup> In classical mechanics, Euler acceleration, also known as azimuthal or transverse acceleration, is the fictitious tangential acceleration that occurs as a result of any change in the radial acceleration. In other words, transverse acceleration occurs when a non-uniformly rotating reference is used for the analysis of motion and when a variation in the angular velocity of the reference frame axes can be observed.

In the CD-like chip, system is restricted to the frame of reference that rotates on a fixed axis. The function of Euler force can be manifested in the liquid filling of the siphon to establish the precondition for the following siphonal flow as well as actuate the siphon valving and liquid extraction. Under the combination of centrifugal and Euler forces, the liquid operation in the siphon valve is performed based on the control of the angular velocity as shown in Fig. 3. In Fig. 3,  $(t_3, t_4)$  is the time interval corresponding to the liquid filling operation occurring in the siphon, where the variation of the angular velocity (i.e., angular acceleration) exists. During the liquid filling, the body forces loaded on the fluid includes the centrifugal force, Euler force, and Coriolis force, respectively, expressed as  $\mathbf{f}_{ce} = \rho\boldsymbol{\omega} \times \mathbf{r} \times \boldsymbol{\omega}$ ,  $\mathbf{f}_{Eu} = -\rho\boldsymbol{\alpha} \times \mathbf{r}$ , and  $\mathbf{f}_{Co} = 2\rho\mathbf{u} \times \boldsymbol{\omega}$ , where  $\rho$  is the fluid density,  $\boldsymbol{\omega}$  is the angular velocity,  $\boldsymbol{\alpha}$  is the angular acceleration equal to  $\frac{d\boldsymbol{\omega}}{dt}$ ,  $\mathbf{r}$  is the rotating radius vector, and  $\mathbf{u}$  is the fluid velocity. The Coriolis force is perpendicular to the fluid velocity, and it does not change the magnitude of fluid velocity but does change its direction. The centrifugal force, in the direction of the rotating radius vector, and the Euler force, in the counterclockwise direction perpendicular to the rotating radius

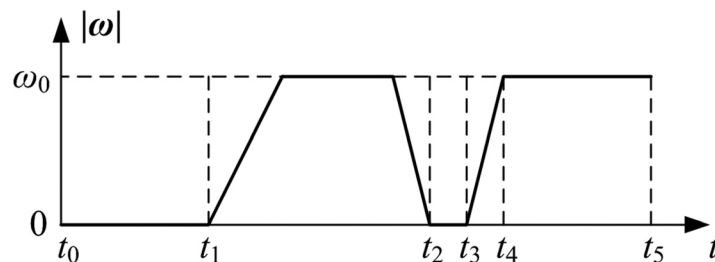


FIG. 3. Schematic for the angular velocity of the liquid operation using siphon valve, where the time intervals  $(t_0, t_1)$ ,  $(t_1, t_2)$ ,  $(t_3, t_4)$ , and  $(t_4, t_5)$ , respectively, correspond to the sampling, metering, filling, and extracting operations.

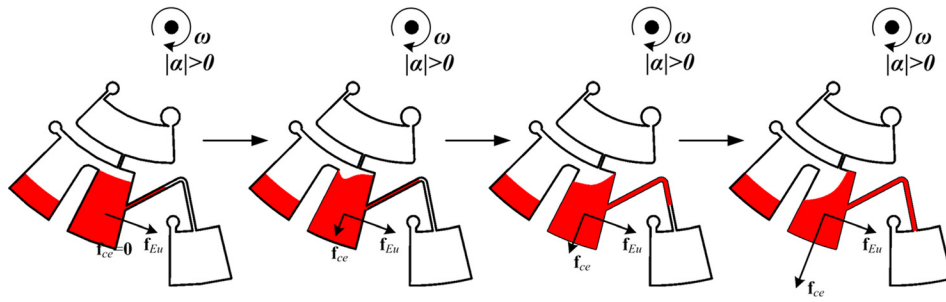


FIG. 4. Schematic for the Euler force actuated liquid filling in the siphon and the evolution of the Euler and centrifugal forces, where the Euler force is the primary driving force compared to the centrifugal force.

vector, can drive the liquid to fill the siphon (Fig. 4). Fig. 4 illustrates the evolution of the Euler and centrifugal forces as time proceeds from  $t_3$  to  $t_4$ . In a short time interval passed the time  $t_3$ , the angular velocity is low, and the ratio of the Euler and centrifugal forces satisfies

$$\frac{|-\rho \boldsymbol{\alpha} \times \mathbf{r}| \cos(\pi/2 - \beta)}{|\rho \boldsymbol{\omega} \times \mathbf{r} \times \boldsymbol{\omega}|} = \frac{|\boldsymbol{\alpha}| \sin \beta}{|\boldsymbol{\omega}|^2} \gg 1, \quad (1)$$

where  $\beta$  is the inclination angle of the siphon channel as depicted in Fig. 1. At present, the Euler force is the primary driving force. Under the action of the Euler force, the liquid surface is tilted in the metering chamber, and the liquid flow in the direction consistent with that of the Euler force is produced. Furthermore, the liquid front in the siphon is driven forward to fill the siphon with the operated liquid. As time progresses, the magnitude of the centrifugal force grows until the ratio of the Euler and centrifugal forces satisfies

$$\frac{|-\rho \boldsymbol{\alpha} \times \mathbf{r}| \cos(\pi/2 - \beta)}{|\rho \boldsymbol{\omega} \times \mathbf{r} \times \boldsymbol{\omega}|} = \frac{|\boldsymbol{\alpha}| \sin \beta}{|\boldsymbol{\omega}|^2} \ll 1. \quad (2)$$

Then the centrifugal force becomes the primary driving force. And it is promoted that the liquid front in the metering chamber recovers to be perpendicular to the rotating radius vector. Extraction of the liquid is conducted continuously based on the siphonal flow primarily driven by the centrifugal force until the liquid surface in the metering chamber reaches the inlet of the siphon (Fig. 5).

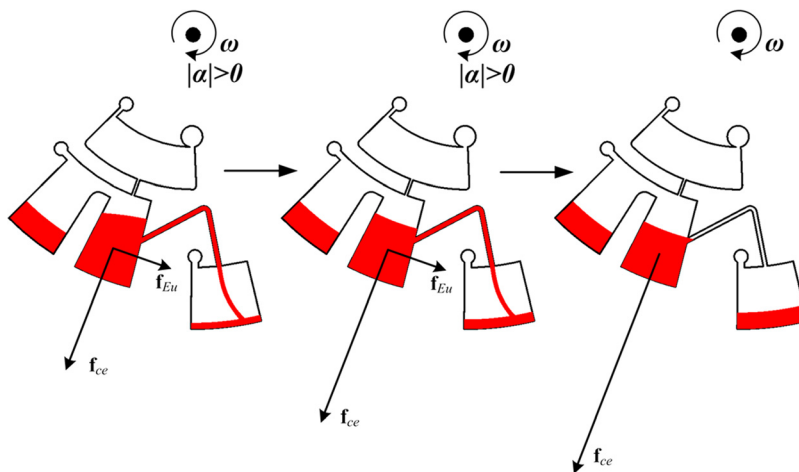


FIG. 5. Schematic for the liquid extraction occurring in the siphon valve and the evolution of the Euler and centrifugal forces, where the centrifugal force becomes the primary driving force compared to the Euler force.

Based on the Euler force produced during the acceleration, the liquid filling of the siphon can be achieved to actuate the siphon valving. Then, the dependence on capillary, surface treatment, and external manipulation of material in the conventional filling of the siphon can be avoided effectively, and the long-term stability of the performance of the CD-like chip can be ensured.

### III. MODELING

To demonstrate the Euler force actuation mechanism for siphon valving, the mathematical modeling is implemented based on the extension of the work of Wang *et al.*<sup>17</sup> and Kim *et al.*<sup>18</sup> The Cartesian coordinate system, with the reference frame fixed on the rotating platform, is adopted. The fluid flow in the siphon valve is the typical two-phase flow formed by the common motion of liquid and air. In this paper, the phase-field method (i.e., diffuse-interface method) is used to describe the two-phase flow by the Cahn–Hilliard equation, where the singularity at the contact line of the two-phase flow is regularized by the Cahn–Hilliard diffusion.<sup>19–21</sup> Under the low Reynolds number characteristic of microfluidics, the fluid motion in the siphon valve is governed by the coupled system including

Stokes equation

$$\rho \frac{\partial \mathbf{u}}{\partial t} = \nabla \cdot [-p\mathbb{I} + \eta(\nabla \mathbf{u} + \nabla \mathbf{u}^T)] + \mu \nabla \phi + \rho \boldsymbol{\omega} \times \mathbf{r} \times \boldsymbol{\omega} - \rho \boldsymbol{\alpha} \times \mathbf{r} + 2\rho \mathbf{u} \times \boldsymbol{\omega}, \quad (3)$$

continuity equation

$$-\nabla \cdot \mathbf{u} = 0, \quad (4)$$

Cahn–Hilliard equation

$$\frac{\partial \phi}{\partial t} + \mathbf{u} \cdot \nabla \phi = \nabla \cdot (M \nabla \mu), \quad (5)$$

and definition of chemical potential

$$\mu = -\nabla \cdot (\lambda \nabla \phi) + \frac{\lambda}{\epsilon^2} \phi (\phi^2 - 1), \quad (6)$$

where  $\rho$  is the fluid density;  $\eta$  is the dynamic viscosity of fluid;  $\mathbf{u}$  and  $p$  are the velocity and pressure, respectively;  $p\mathbb{I}$  is the pressure tensor;  $\epsilon$  is the capillary width, which is the physical measurement of the thickness of the diffusive interface between two fluids;  $\lambda$  is the mixing energy density, which is determined according to the relation between the mixing energy density and surface tension  $\sigma = \frac{2\sqrt{2}\lambda}{3\epsilon}$ ;  $M$  is the mobility or Onsager coefficient, which determines the time scale of the Cahn–Hilliard diffusion and must be large enough to retain a constant interfacial thickness but small enough so that the convective terms are not overly damped;  $\phi$  is the phase-field variable, satisfying the two-phase bulks  $\phi = \pm 1$ ; the two-phase interface is given by  $\phi = 0$ ;  $\mu$  is the chemical potential;  $\mu \nabla \phi$  is the capillary force, which is the diffuse-interface equivalent of the interfacial tension;<sup>22</sup>  $\rho \boldsymbol{\omega} \times \mathbf{r} \times \boldsymbol{\omega}$ ,  $-\rho \boldsymbol{\alpha} \times \mathbf{r}$ , and  $2\rho \mathbf{u} \times \boldsymbol{\omega}$  are, respectively, the centrifugal force, Euler force, and Coriolis force, as explained in Sec. II. The density and dynamic viscosity are functions of the phase-field variable

$$\begin{aligned} \rho &= \rho_a + (\rho_l - \rho_a) \min \left( \max \left( \frac{\phi + 1}{2}, 0 \right), 1 \right), \\ \eta &= \eta_a + (\eta_l - \eta_a) \min \left( \max \left( \frac{\phi + 1}{2}, 0 \right), 1 \right), \end{aligned} \quad (7)$$

where  $\rho_a$  and  $\eta_a$  are the density and dynamic viscosity of air;  $\rho_l$  and  $\eta_l$  are the density and dynamic viscosity of the considered liquid. The initial and boundary conditions of the coupled system are set as follows: initial condition

$$\begin{aligned}\mathbf{u}(t=0) &= \mathbf{u}_0, \\ \phi(t=0) &= \phi_0,\end{aligned}\quad (8)$$

initial interface

$$\phi_0 = 0, \quad (9)$$

boundary condition at the inlet

$$\begin{aligned}[-p\mathbb{I} + \eta(\nabla\mathbf{u} + \nabla\mathbf{u}^T)] \cdot \mathbf{n} &= \mathbf{0}, \\ \mathbf{n} \cdot M\nabla\mu &= 0, \\ \phi &= -1,\end{aligned}\quad (10)$$

boundary condition at the wall

$$\begin{aligned}\mathbf{u} &= \mathbf{0}, \\ \mathbf{n} \cdot M\nabla\mu &= 0, \\ \lambda\mathbf{n} \cdot \nabla\phi &= \frac{3}{4}\sigma(1 - \phi^2)\cos\theta,\end{aligned}\quad (11)$$

boundary condition at the open boundary

$$\begin{aligned}[-p\mathbb{I} + \eta(\nabla\mathbf{u} + \nabla\mathbf{u}^T)] \cdot \mathbf{n} &= \mathbf{0}, \\ \mathbf{n} \cdot M\nabla\mu &= 0, \\ \lambda\mathbf{n} \cdot \nabla\phi &= 0,\end{aligned}\quad (12)$$

where  $\mathbf{u}_0$  and  $\phi_0$  represent the initial distribution of the fluid velocity and phase-field variable, respectively;  $\theta$  is the contact angle of the liquid on the wall boundary;  $\mathbf{n}$  is the outward unit norm vector;  $\mathbf{n} \cdot M\nabla\mu$  and  $\lambda\mathbf{n} \cdot \nabla\phi$ , respectively, represent the normal diffusive flux of the chemical potential and mixing energy. As the realistic material surface has roughness and chemical inhomogeneity, the contact angle deviates from the equilibrium value when the contact line moves. The difference between the advancing and receding contact angles is referred to as the hysteresis of contact angle.<sup>27–29</sup> In this paper, the hysteresis of contact angle is considered according to Ref. 29.

In the above, the Cahn-Hilliard equation describes the convection-diffusion of the phase field of the two-phase flow.  $\frac{\partial\phi}{\partial t} + \mathbf{u} \cdot \nabla\phi$ , the material derivative of the phase field, describes the action of fluid convection on the phase field; and  $\nabla \cdot (M\nabla\mu)$ , the diffusion of chemical potential, represents the action of the diffusive flux proportional to the gradient of chemical potential. The chemical potential is obtained by minimizing the total free energy of a system with nominally immiscible fluids in contact with a solid surface. Based on the variational procedure of the total free energy,<sup>21,23</sup> the chemical potential (Eq. (6)), capillary force in Eq. (3), and the boundary conditions of the phase field (Eqs. (10)–(12)) can be obtained. On more details of the phase-field method and Cahn-Hilliard equation, one can refer to Refs. 19–24.

#### IV. NUMERICAL ANALYSIS

Numerical solution of the coupled system is conducted using the finite element method to investigate the flow characteristics and Euler force actuation mechanism for siphon valving. The finite element solution is implemented using the commercial software COMSOL

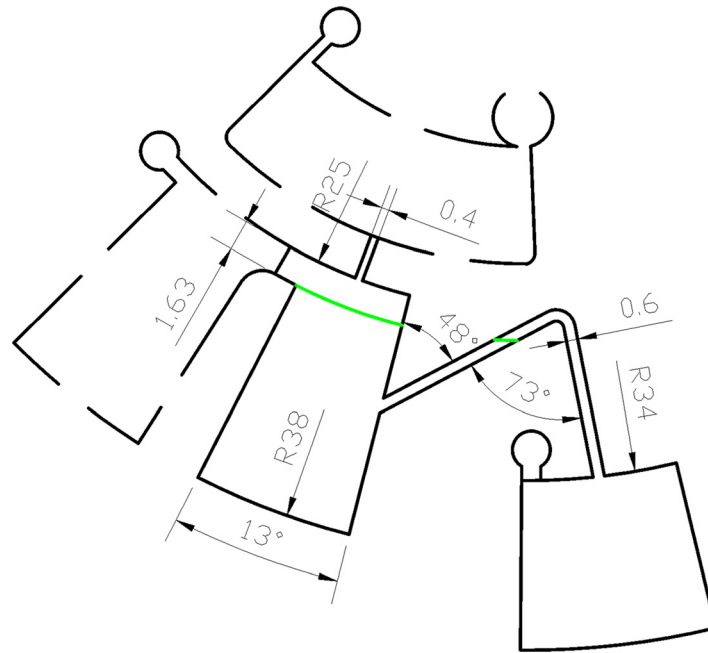


FIG. 6. Size of the geometry for the siphon valve simulated in this paper, where the chambers with dashed line are removed to reduce the computation cost and the green line represents the initial liquid surface.

Multiphysics 3.5 (<http://www.comsol.com>), where the numerical implementation is based on the basic module of the software: *COMSOL Multiphysics*  $\rightarrow$  *PDE Modes*  $\rightarrow$  *PDE, General Form*. In the numerical implementation, Taylor–Hood elements are used for the Stokes equations, where the fluid velocity and pressure are, respectively, interpolated quadratically and linearly;<sup>30</sup> and the Cahn–Hilliard equations are solved using quadratic elements in which the phase-field variable and chemical potential are both interpolated quadratically.

The numerical analysis is conducted in the 2D geometry shown in Fig. 6 in which only the metering chamber and siphon are included to reduce the computational cost. The inclination angle of the siphon channel is  $\beta = 48^\circ$ . The geometry in Fig. 6 is meshed using triangular elements. The initial time is set to be  $t_3 = 0$ ; the initial distribution of the fluid velocity is set to be  $\mathbf{u}_0 = 0$  in Eq. (8); the initial liquid surface is set to be the green line shown in Fig. 6, and the reference pressure is set to be zero in the simulations. The liquid considered is water and the physical parameters of the fluid are listed in Table I.

## V. EXPERIMENTS

To confirm the validity of the Euler force actuation mechanism for siphon valving, the CD-like microfluidic chips with siphon valves shown in Fig. 1 are manufactured and tested. In experiments, standard CAD software was used in designing the CD-like chips. The multi-layer polymer substrates featuring the 100 mm diameter disc format was manufactured through the following prototyping techniques: (1) the microfluidic structures and one mounting hole are machined in 1 mm thick polymethylmethacrylate (PMMA; SPOLYTECH, Korea) using a CO<sub>2</sub> laser engraving system (TROTEC, Speedy 100R, Austria) in which both sides of the polymer are stuck with 250  $\mu\text{m}$ -thick pressure-sensitive adhesive (PSA) layers (HAOXIANG, China);

TABLE I. Parameters used in the numerical analysis of the Euler force actuation mechanism.

$\rho_l(\text{kg/m}^3)$	$\rho_a(\text{kg/m}^3)$	$\eta_l(\text{Pa s})$	$\eta_a(\text{Pa s})$	$\sigma(\text{N/m})$	$M(\text{m}^2 \text{s/kg})$	$\epsilon(\text{m})$	$\theta$
$1 \times 10^3$	$1.21 \times 10^0$	$1 \times 10^{-3}$	$1.8 \times 10^{-5}$	$7.3 \times 10^{-2}$	$1 \times 10^2$	$2 \times 10^{-4}$	$70^\circ$

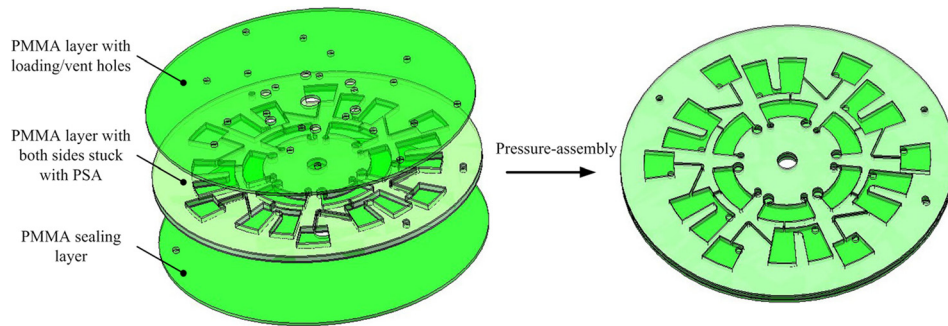


FIG. 7. Schematic for the pressure-assembly of the manufactured PMMA layers.

(2) the CO<sub>2</sub> laser engraving system was used to manufacture the PMMA disc with 100 mm diameter and 0.8 mm thickness as well as sample inlets, air vents, and mounting hole; (3) the CO<sub>2</sub> laser engraving system was used to manufacture the PMMA disc used as the sealing layer and with 100 mm diameter and 0.8 mm thickness, as well as one mounting hole; (4) the obtained PMMA discs are pressure-assembled based on the adhesion of the PSA layers to

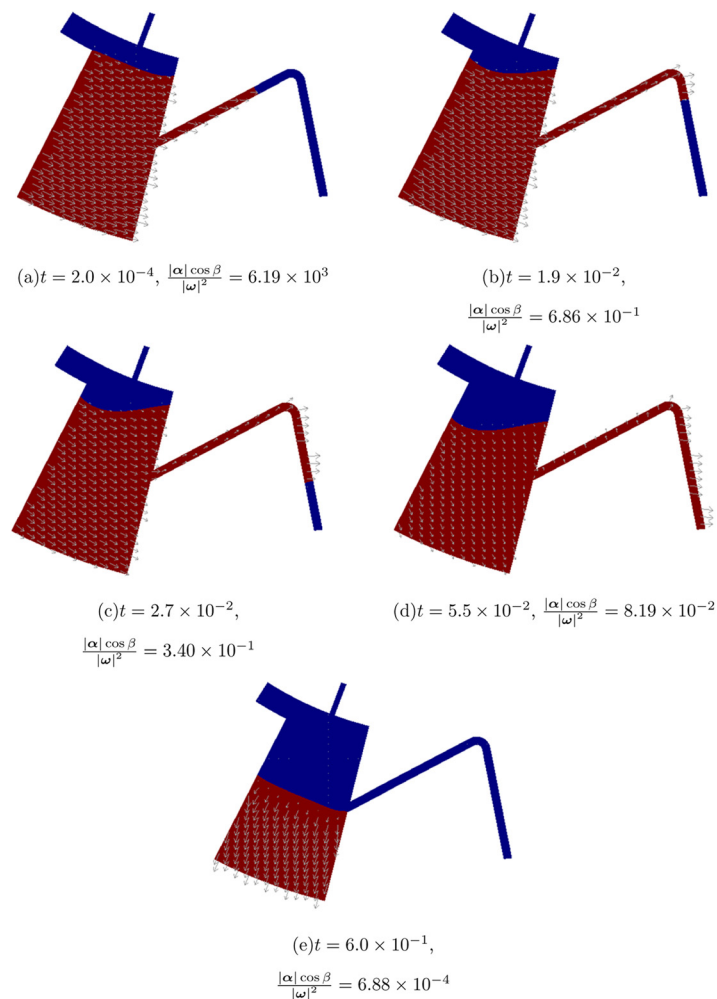


FIG. 8. Snapshots for the evolution of the direction of the body force and liquid surface in the Euler force actuated siphon valve.

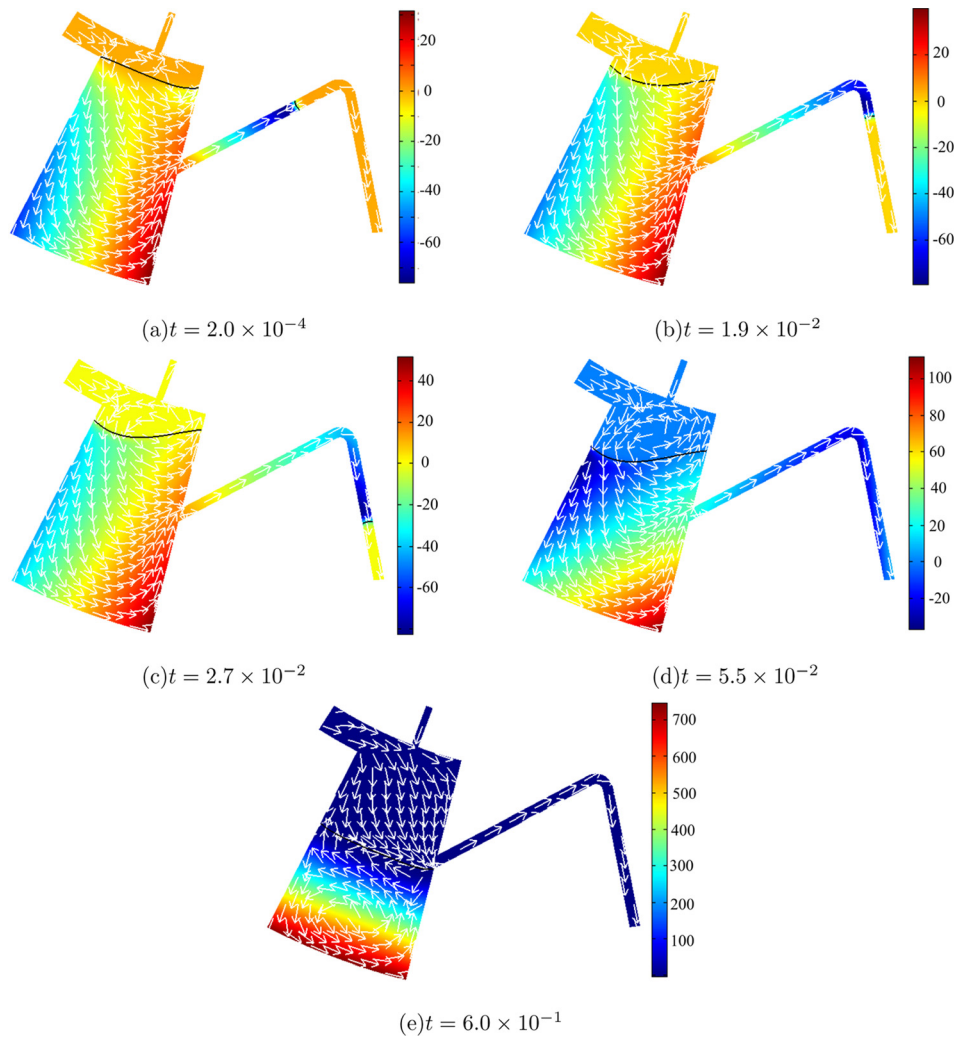


FIG. 9. Snapshots for the evolution of the pressure distribution and normalized velocity vectors in the Euler force actuated siphon valve (the unit of pressure is Pa).

enclose the top and bottom sides of the structures manufactured in the first step. The pressure-assembly of the three-layer CD-like chip is illustrated in Fig. 7.

The manufactured CD-like chip is mounted on the axle of the rotating platform and red-colored dye (Neon food dye, McCormick, US) is injected into the chip from the sample inlets. Then, the chip is rotated at the angular velocity as depicted in Fig. 3. To record the liquid operation progress in the siphon valve, high-resolution imaging during fast rotation was video captured at 4000 frames/s using a high speed camera (i-speed TR, Olympus Corporation, Japan). The pictures are exported by i-SPEED software suite.

Table II. List of the time cost for the liquid filling of the siphon valve with different inclination angles under different angular accelerations.

	750 rpm/s	1500 rpm/s	3000 rpm/s
12°	0.0364 s	0.0340 s	0.0308 s
24°	0.0370 s	0.0344 s	0.0312 s
36°	0.0386 s	0.0356 s	0.0320 s
48°	0.0432 s	0.0390 s	0.0334 s

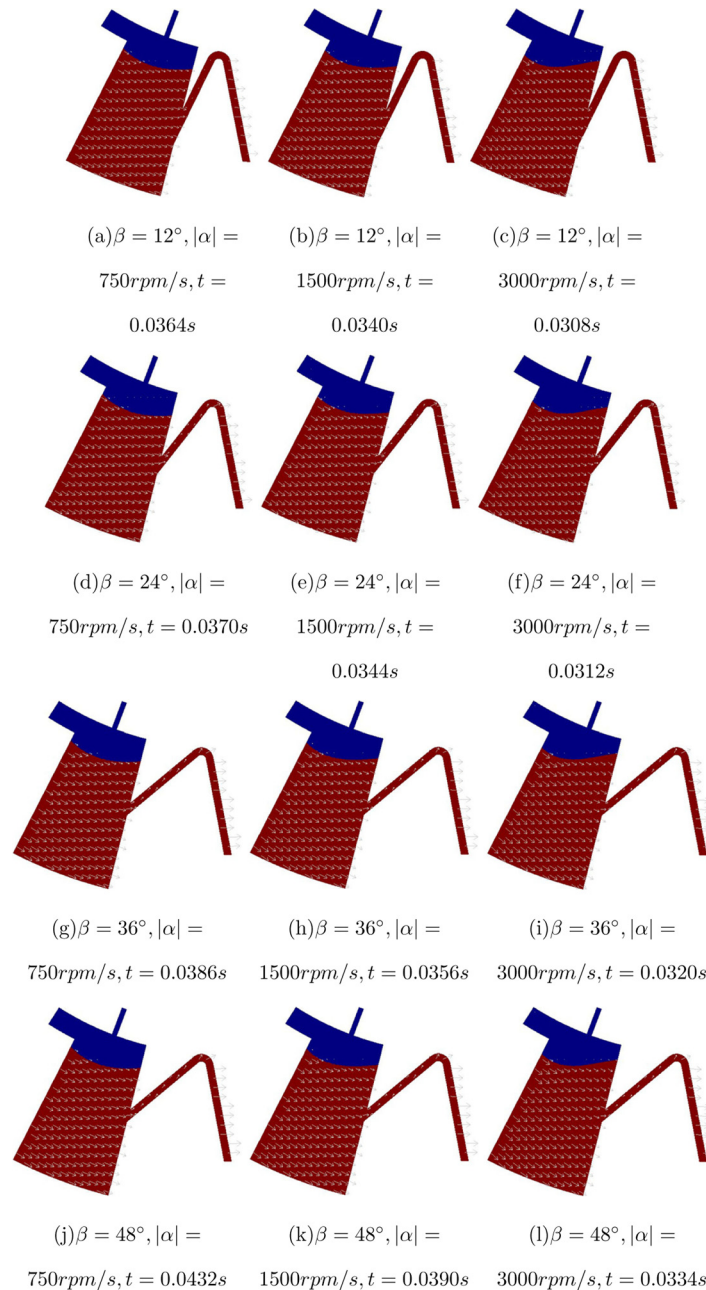


FIG. 10. The phase field distribution corresponding to the time listed in Table II, where the gray arrows represent the direction of the body force.

## VI. RESULTS AND DISCUSSION

### A. Numerical results

Based on the numerical analysis introduced in Sec. IV, the Euler force actuation mechanism for siphon valving is revealed by solving the coupled system of the Stokes and Cahn–Hilliard equations in the 2D geometry shown in Fig. 6, where the angular acceleration 3000rpm/s is used to accelerate the system from 0 to 3000rpm.

On the Euler force actuation mechanism for siphon valving, it is essential to understand how the Euler force drives the liquid to fill the siphon. Therefore, snapshots for the body force

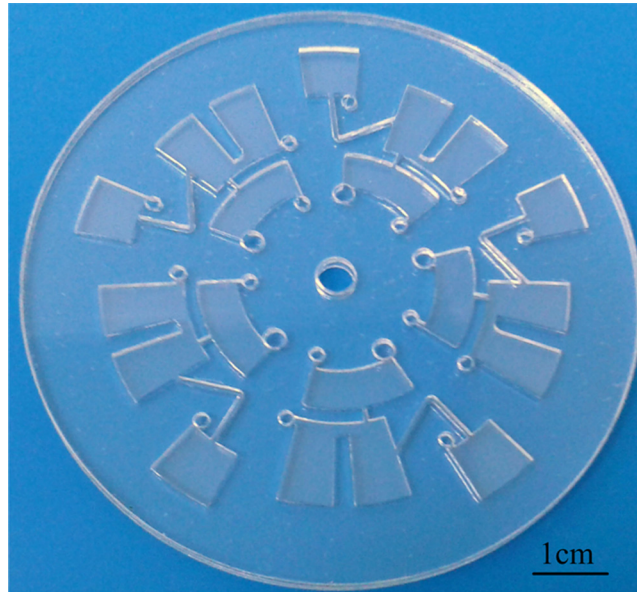


FIG. 11. CD-like microfluidic chip, with Euler force actuated siphon valves, used in experiments.

are presented in Fig. 8, and the induced pressure distribution and normalized velocity vectors are presented in Fig. 9. The negative pressure is presented in the snapshots of the pressure distribution (Fig. 9). During the preliminary acceleration stage, the counterclockwise Euler force results in the negative pressure in the siphon valve, where the Euler force takes the primary place compared with the centrifugal and Coriolis forces. Then, the pressure difference between the metering chamber and the siphon microchannel is induced by the negative pressure. From the normalized velocity vectors, one conforms that the liquid flows from the higher pressure area to the low pressure area, i.e., suction flow driven by the pressure difference occurs in the siphon valve, where the suction of the liquid based on the negative pressure has been discussed elsewhere.<sup>8</sup> This pressure difference drives the suction flow that fills the siphon until the siphonal flow is actuated. As time progresses, the primary place of the Euler force is changed and the centrifugal force becomes primary to allow continuous siphonal flow. The primary place of the centrifugal force at the later stage of acceleration can ensure precise volume of the extracted liquid.

For the effect of the inclination angle on siphon valving operation, the siphon valve with different inclination angles are simulated under different angular accelerations. The time cost of the liquid filling is recorded as listed in Table II. And the phase field distribution corresponding to the time listed in Table II is shown in Fig. 10. The crest points of siphon valves in Fig. 10 have the same rotation radius. The datum in Table II and Fig. 10 demonstrates that higher angular acceleration corresponds to lower time cost for the liquid filling of the siphon in the siphon valve with the same inclination angle, because higher angular acceleration produces larger Euler force at the preliminary acceleration stage; higher time cost for the liquid filling of the siphon corresponds to larger inclination angle, because larger inclination angle of the siphon valve means longer siphon microchannel.

## B. Experimental results

Using the experimental method introduced in Sec. V, experiments were conducted to validate the Euler force actuation mechanism proposed in Sec. II and demonstrated by the numerical analysis in Sec. VI A. The CD-like microfluidic chip with Euler force actuated siphon valves was manufactured as shown in Fig. 11. The experiments were performed by transferring first 100  $\mu\text{l}$  loaded dye into the metering and waste chambers at a maximum rotational speed of

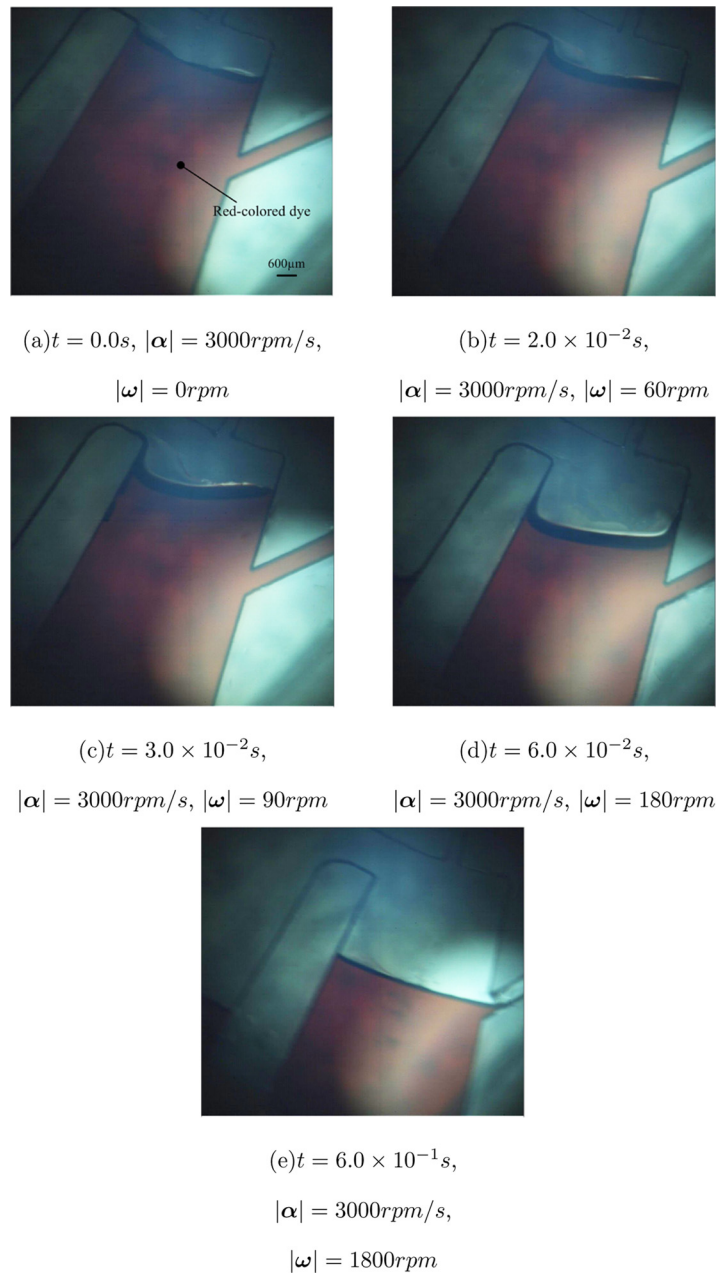


FIG. 12. Snapshots for the evolution of the liquid surface in the metering chamber during the acceleration of the CD-like microfluidic chip. Under the action of the Euler force, the liquid surface is tilted in the metering chamber and the liquid flow in the direction consistent with that of the Euler force is produced. Furthermore, the liquid front in the siphon is driven forward to fill the siphon.

4000 rpm for 30 s. Subsequently, the CD-like chip was accelerated with the angular acceleration 3000 rpm/s to a maximum rotational speed of 3000 rpm, and 30  $\mu$ l of the loaded dye was extracted. During the acceleration progress, the liquid surface in the metering chamber and positions of the liquid front in the siphon were visually recorded with the high speed camera. After image acquisition, movie frames were extracted to show the position of the liquid surface and front (Figs. 12 and 13).

From experimentally recorded proceeding of the liquid surface in the metering chamber (Fig. 12) and the liquid front in the siphon microchannel (Fig. 13), one can conform the suction flow induced by the negative pressure in the siphon microchannel. Furthermore, the Euler force

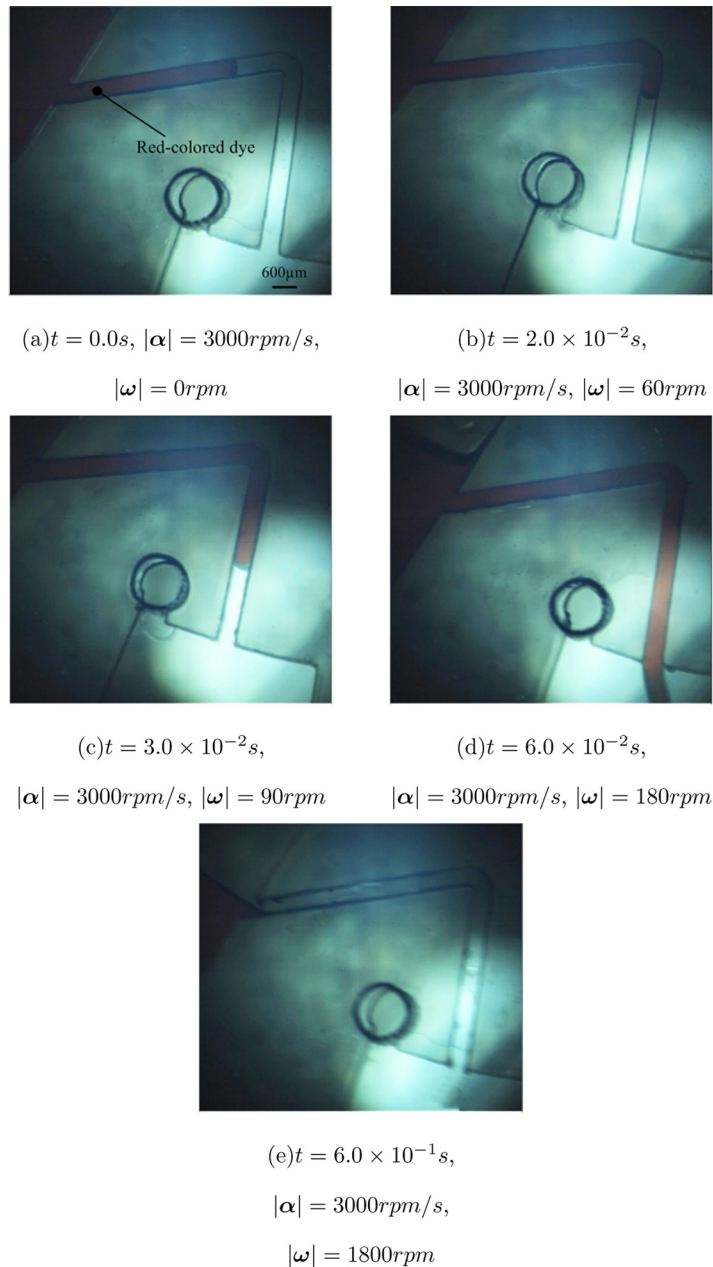


FIG. 13. Snapshots for the evolution of the liquid front in the siphon during the acceleration of the CD-like microfluidic chip. Under the action of the Euler force, the liquid front in the siphon is driven forward to fill the siphon and the siphon flow is actuated to extract the liquid in the metering chamber.

actuation mechanism for siphon valving can be identified. The Euler force actuation mechanism provides a novel method for pumping liquids back to the center of the CD-like chip without using external pumping manipulation or capillary based on surface treatments. Current centrifugal platforms, particularly integrated CD-based *in vitro* diagnostic devices, use surface treatments to implement siphon valving.<sup>2,5,25,26</sup> These siphon microchannels are typically treated by a plasma cleaner, but the induced hydrophilicity changes over time. To avoid surface treatments, Madou *et al.* has proposed the pneumatic pumping technique.<sup>6</sup> In addition, the pneumatic pumping technique has been applied to the comprehensive integration of homogeneous bioassays achieved by Ducrée *et al.*<sup>4</sup> However, the pneumatic pumping technique has typically prevented highly integrated processing because of the need of the volume-occupied compressed

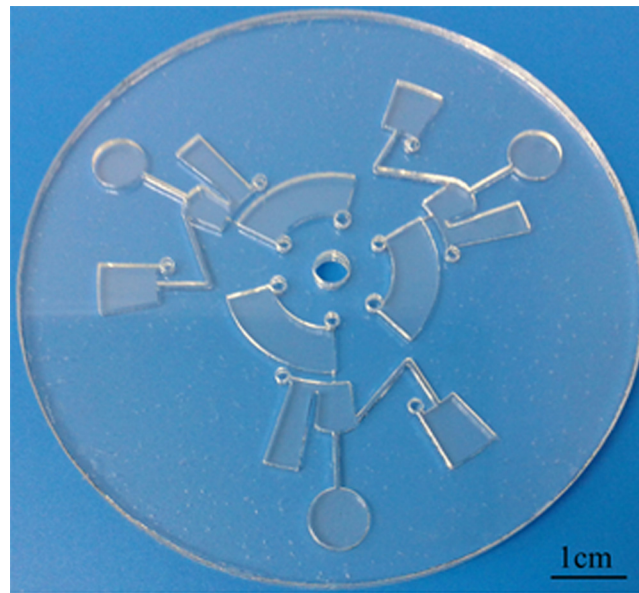


FIG. 14. CD-like microfluidic chip used for whole blood separation and plasma extraction.

air chamber. The Euler force actuation mechanism avoids the surface treatments effectively and overcomes the limitation of pneumatic pumping technique by excluding the additional compressed air chamber. Therefore, it is a valuable attempt to integrate the Euler force actuated siphon valve in future CD-like microfluidic chips.

## VII. APPLICATION: WHOLE BLOOD SEPARATION AND PLASMA EXTRACTION

To prove the application for biological samples, whole blood separation and plasma extraction are conducted using the Euler force actuation mechanism proposed in this paper. Whole blood analysis has been implemented using the CD-like microfluidic chip.<sup>4,32,33</sup> In these researches, whole blood separation and plasma extraction were implemented based on the

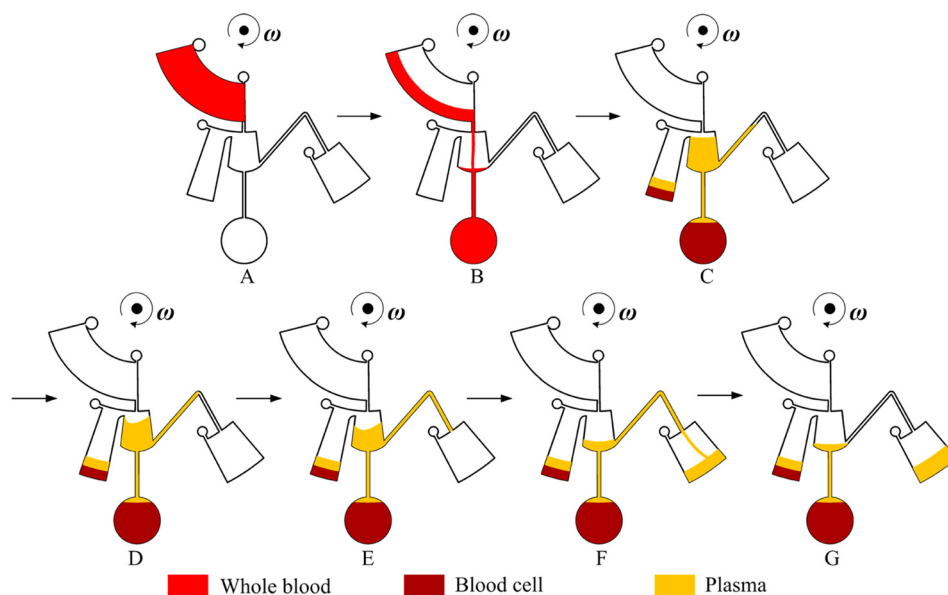


FIG. 15. Schematic for the whole blood separation and plasma extraction in the CD-like chip.

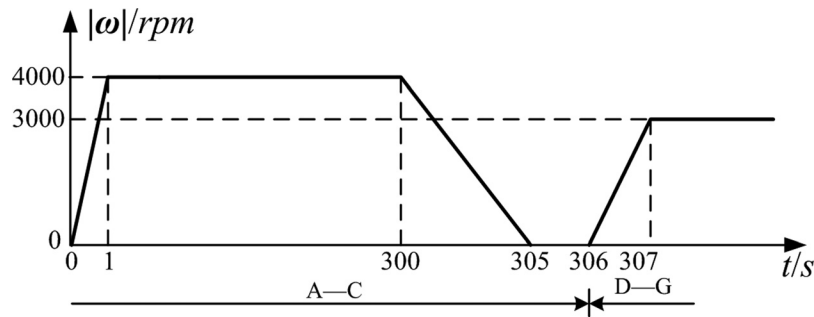


FIG. 16. Schematic for rotating speed used in the whole blood separation and plasma extraction.

siphon valving, where the flowing back of the liquid to the disc center was achieved based on the capillary depending on hydrophilic surface treatment or pneumatic pumping technique with volume-occupied compressed air chamber.

In this section, the CD-like microfluidic chip, used for whole blood separation and plasma extraction, is manufactured as shown in Fig. 14. In Fig. 14, the metering chamber is redesigned for whole blood separation and plasma extraction, where a microchannel is used to connect the two parts which are, respectively, used to load plasma and blood cells. The design of the metering chamber can prevent the remixing of the separated blood cells and plasma, where the remixing is induced by releasing elastic potential energy stored in the separated blood cells at

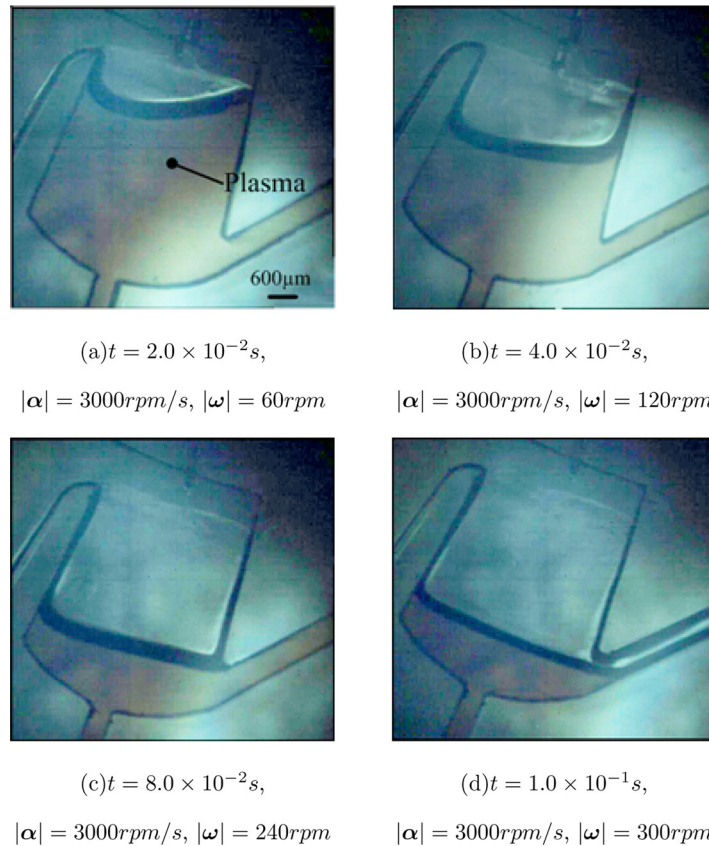


FIG. 17. Snapshots for the evolution of the plasma surface in the metering chamber during the acceleration of the CD-like microfluidic chip. Under the action of the Euler force, the plasma surface is tilted in the metering chamber and the plasma front in the siphon is driven forward to fill the siphon. Furthermore, the siphon valve is actuated and the plasma is extracted from the metering chamber.

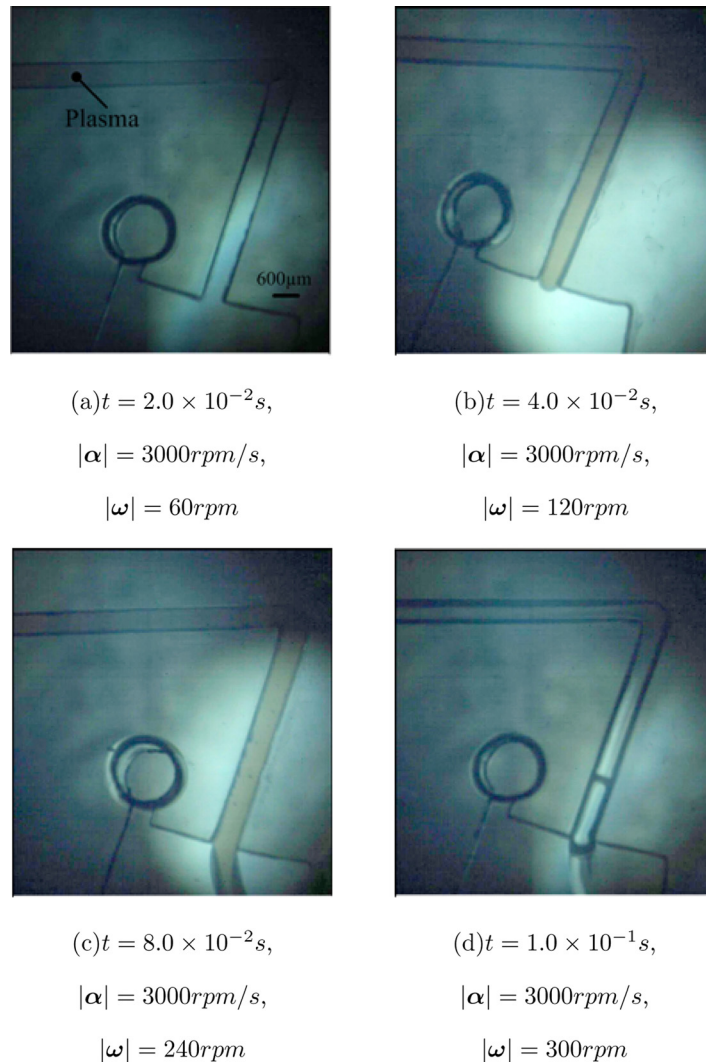


FIG. 18. Snapshots for the evolution of the plasma front in the siphon during the acceleration of the CD-like microfluidic chip, where the plasma is driven to fill the siphon and actuate the siphon valving.

the end of the blood separation operation.<sup>31</sup> The CD-like chip is operated as shown in Figs. 15 and 16, where  $160 \mu l$  of the whole blood was placed on the chip and  $35 \mu l$  of the separated plasma was extracted. The blood separation is conducted with rotating speed of 4000 rpm for 300 s after filling the sample chamber with whole blood. Consequently, the angular acceleration 3000 rpm/s is imposed until the rotating speed reaches 3000 rpm. Based on the aforementioned operation, the Euler force, induced by the imposed angular acceleration, actuated the siphon valving and achieved the plasma extraction in which the evolution of the liquid surface in the metering chamber and liquid front in the siphon were recorded as shown in Figs. 17 and 18. The results confirm the flowing back of the separated plasma to the center of the CD-like chip, thereby achieving the whole blood separation and plasma extraction. Therefore, the effectiveness of the Euler force actuation mechanism for biological samples can be demonstrated during the siphon valving operation of whole blood in the CD-like microfluidic chip.

## VIII. CONCLUSIONS

This paper proposes the Euler force actuation mechanism for siphon valving in CD-like microfluidic chips. Based on the mathematical modeling of the Euler force actuated siphon

valving and corresponding numerical analysis, the Euler force actuation mechanism for siphon valving is revealed. At the preliminary stage of the acceleration of CD-like chip, the Euler force takes the primary place compared with the centrifugal and Coriolis forces, and the primary Euler force in tangential direction induces the negative pressure and pressure difference between the metering chamber and siphon. This pressure difference drives the flow that achieves the siphon filling to actuate the siphonal flow. The validity of the Euler force actuation mechanism is proven experimentally using the chips fabricated by CO<sub>2</sub> laser engraving technique. Application of the Euler force actuation mechanism for siphon valving is provided for the whole blood separation and plasma extraction. Experimental results indicate that the Euler force actuation mechanism can be utilized in the operation of biological samples on the CD-like platform.

The proposed Euler force actuation mechanism can help the siphon valve to be independent on capillary filling of the siphon, prevent hydrophilic surface treatment, and ensure long-term stability of the CD-like microfluidic chip manufactured using polymeric material with inherent hydrophobicity. The Euler force actuation mechanism can also overcome the typical impracticality on highly integration encountered as pneumatic pumping technique is used to pump the liquid to the center of the CD-like chip. Therefore, the long-term stable CD-like chips can be mass-produced using polymeric material and Euler force based actuation.

The liquid front passing the crest point before the centrifugal force becoming dominant is key for the liquid operation in the Euler force actuation mechanism. For one given design of the siphon valve, the liquid filling of the siphon can be achieved by choosing an angular acceleration large enough, because large angular acceleration means large Euler force. Then large Euler force can ensure the liquid front passing the crest point before the centrifugal force becoming dominant, especially for the case where the siphon is hydrophobic and capillary cannot occur at all.

In addition, the Euler force actuation mechanism is short in duration and increases the operation complexity. Moreover, the active time for the Euler force is discounted if the CD-like chip is already in motion, e.g., to maximize the Euler force, a 4000 rpm/s high acceleration is used. If the maximum angular velocity of the system is 4000 rpm, then the Euler force is applied at 1 s; and if the disc is already in motion, the useful force can be applied for only a fraction of 1 s.

## ACKNOWLEDGMENTS

This work was supported by the National Natural Science Foundation of China (Nos. 11034007, 50975272, and 51205381), the National High Technology Program of China (863 Program, No. 2012AA040503), and the Open Fund of SKLAO. The authors are grateful to the reviewers' kind attention and valuable suggestions.

- <sup>1</sup>J. V. Zoval and M. J. Madou, "Centrifuge-based fluidic platforms," *Proc. IEEE* **92**, 140–153 (2004).
- <sup>2</sup>J. Ducreé, S. Haerberle, S. Lutz, S. Pausch, F. von Stetten, and R. Zengerle, "The centrifugal microfluidic Bio-Disk platform," *J. Micromech. Microeng.* **17**, 103–115 (2007).
- <sup>3</sup>R. Gorkin, J. Park, J. Siegrist, M. Amasia, B. S. Lee, J. M. Park, J. Kim, H. Kim, M. Madou, and Y. K. Cho, "Centrifugal microfluidics for biomedical applications," *Lab Chip* **10**, 1758–1773 (2010).
- <sup>4</sup>N. Godino, R. Gorkin III, A. V. Linares, R. Burgera, and J. Ducreé, "Comprehensive integration of homogeneous bioassays via centrifugo-pneumatic cascading," *Lab Chip* **13**, 685 (2013).
- <sup>5</sup>J. Steigert, T. Brenner, M. Grumann, L. Riegger, S. Lutz, R. Zengerle, and J. Ducreé, "Integrated siphon-based metering and sedimentation of whole blood on a hydrophilic lab-on-a-disk," *Biomed. Microdevices* **9**, 675–679 (2007).
- <sup>6</sup>R. Gorkin III, L. Clime, M. Madou, and H. Kido, "Pneumatic pumping in centrifugal microfluidic platforms," *Microfluid. Nanofluid.* **9**, 541–549 (2010).
- <sup>7</sup>Z. Noroozi, H. Kido, M. Micic, H. Pan, C. Bartolome, M. Princevac, J. Zoval, and M. Madou, "Reciprocating flow-based centrifugal microfluidics mixer," *Rev. Sci. Instrum.* **80**, 075102 (2009).
- <sup>8</sup>R. Gorkin, S. Soroori, W. Southard, L. Clime, T. Veres, H. Kido, L. Kulinsky, and M. Madou, "Suction-enhanced siphon valves for centrifugal microfluidic platforms," *Microfluid. Nanofluid.* **12**, 345 (2012).
- <sup>9</sup>C. H. Shih, C. H. Lu, W. L. Yuan, W. L. Chiang, and C. H. Lin, "Supernatant decanting on a centrifugal platform," *Biomicrofluidics* **5**, 013414 (2011).
- <sup>10</sup>M. Focke, F. Stumpf, G. Roth, R. Zengerle, and F. Stetten, "Centrifugal microfluidic system for primary amplification and secondary real-time PCR," *Lab Chip* **10**, 3210–3212 (2010).
- <sup>11</sup>M. C. R. Kong and E. D. Salin, *Anal. Chem.* **82**, 8039–8041 (2010).

- <sup>12</sup>K. Abi-Samra, L. Clime, L. Kong, R. Gorkin III, T. H. Kim, Y. K. Cho, and M. Madou, *Microfluid. Nanofluid.* **11**, 643–652 (2011).
- <sup>13</sup>Z. Noroozi, H. Kido, and M. J. Madou, *J. Electrochem. Soc.* **158**, 130–135 (2011).
- <sup>14</sup>W. Al-Faqheri, F. Ibrahim, T. H. G. Thio, J. Moebius, K. Joseph, H. Arof, and M. Madou, “Vacuum/compression valving (VCV) using paraffin-wax on a centrifugal microfluidic CD platform” *PLoS ONE* **8**(3), e58523 (2013).
- <sup>15</sup>M. Amasia, S. W. Kang, D. Banerjee, and M. Madou, “Experimental validation of numerical study on thermoelectric-based heating in an integrated centrifugal microfluidic platform for polymerase chain reaction amplification,” *Biomicrofluidics* **7**, 014106 (2013).
- <sup>16</sup>G. K. Batchelor, *An Introduction to Fluid Dynamics* (Cambridge University Press, Cambridge, 1967).
- <sup>17</sup>L. Wang, M. C. Kropinski, and P. C. H. Li, “Analysis and modeling of flow in rotating spiral microchannels: Towards math-aided design of microfluidic systems using centrifugal pumping,” *Lab Chip* **11**, 2097–2108 (2011).
- <sup>18</sup>D. S. Kim and T. H. Kwon, “Modeling, analysis and design of centrifugal force-driven transient filling flow into a circular microchannel,” *Microfluid. Nanofluid.* **2**, 125–140 (2006).
- <sup>19</sup>J. W. Cahn and J. Hilliard, “Free energy of a nonuniform system. I. Interfacial free energy,” *J. Chem. Phys.* **28**, 258–267 (1958).
- <sup>20</sup>D. M. Anderson, G. B. McFadden, and A. A. Wheeler, “Diffuse-interface methods in fluid mechanics,” *Annu. Rev. Fluid Mech.* **30**, 139–165 (1998).
- <sup>21</sup>D. Jacqmin, “Contact-line dynamics of a diffuse fluid interface,” *J. Fluid Mech.* **402**, 57–88 (2000).
- <sup>22</sup>P. Yue, C. Zhou, J. J. Feng, C. F. Ollivier-Gooch, and H. H. Hu, “Phase-field simulations of interfacial dynamics in visco-elastic fluids using finite elements with adaptive meshing,” *J. Comput. Phys.* **219**, 47–67 (2006).
- <sup>23</sup>T. Qian, X. P. Wang, and P. Sheng, “Molecular hydrodynamics of the moving contact line in two-phase immiscible flows,” *Commun. Comput. Phys.* **1**, 1–52 (2006).
- <sup>24</sup>J. Kim, “Phase-field models for multi-component fluid flows,” *Commun. Comput. Phys.* **12**, 613–661 (2012).
- <sup>25</sup>See [www.abaxis.com](http://www.abaxis.com) for Abaxis, Inc., USA (2009).
- <sup>26</sup>H. Kido, M. Micic, D. Smith, J. Zoval, J. Norton, and M. Madou, “A novel, compact disk-like centrifugal microfluidics system for cell lysis and sample homogenization,” *Colloids Surf. B* **58**, 44–51 (2007).
- <sup>27</sup>R. L. Hoffman, “A study of the advancing interface. I. Interface shape in liquid-gas systems,” *J. Colloid Interface Sci.* **50**, 228–241 (1975).
- <sup>28</sup>E. B. Dussan, “On the spreading of liquids on solid surfaces: Static and dynamic contact lines,” *Annu. Rev. Fluid Mech.* **11**, 371–400 (1979).
- <sup>29</sup>S. Ganesan, “On the dynamic contact angle in simulation of impinging droplets with sharp interface methods,” *Microfluid. Nanofluid.* **14**, 615–625 (2013).
- <sup>30</sup>H. C. Elman, D. J. Silvester, and A. J. Wathen, *Finite Elements and Fast Iterative Solvers: With Applications in Incompressible Fluid Dynamics* (Oxford University Press, Oxford, 2006).
- <sup>31</sup>T. J. Li, L. M. Zhang, M. L. Kar *et al.*, “Out-of-plane microvalves for whole blood separation on lab-on-a-CD,” *J. Micromech. Microeng.* **20**, 105024 (2010).
- <sup>32</sup>B. S. Lee, Y. U. Lee, H. S. Kim, T. H. Kim, J. Park, J. G. Lee, J. Kim, H. Kim, W. G. Lee, and Y. K. Cho, “Fully integrated lab-on-a-disc for simultaneous analysis of biochemistry and immunoassay from whole blood,” *Lab Chip* **11**, 70–78 (2011).
- <sup>33</sup>J. Steigert, M. Grumann, T. Brenner, L. Riegger, J. Harter, R. Zengerlea, and J. Ducrée, “Fully integrated whole blood testing by real-time absorption measurement on a centrifugal platform,” *Lab Chip* **6**, 1040–1044 (2006).